

MULTISCALE MECHANISMS OF SRF BREAKDOWN

A. Gurevich

Applied Superconductivity Center, University of Wisconsin, Madison, WI 53706, U.S.A.

Abstract

Multiscale mechanisms of SRF breakdown and the dependence of the quality factor $Q(H_0)$ on the rf field amplitude H_0 are discussed. We first consider a basic nonlinear dependence of the surface resistance R_s on the rf screening current density J , which becomes crucial at rf field of the order of the thermodynamic critical field $H_c^{Nb} \sim 200$ mT. The current-induced rf pairbreaking in the clean limit results in a quadratic field correction to $R_s(H_0)$ at low H_0 and an exponential increase of $R_s(H_0)$ at $H_0 > TH_c/T_c$. The effect of the nonlinear $R_s(H_0)$ on the rf thermal breakdown is addressed. The field dependence of $R_s(H_0)$ reduces the breakdown field H_b below H_c and increases the medium and high field Q slopes. Then a model of nonuniform thermal breakdown caused by macroscopic hotspots on the cavity surface is proposed. It is shown that hotspots expand as H_0 increases, resulting in additional mechanism of field dependence of $Q(H_0)$, which increases the Q slope and reduces H_b .

INTRODUCTION

The quality factor $Q = G/R_s$ of high performance superconducting cavities for particle accelerators is determined by the small surface resistance R_s at low temperatures T for which the role of extrinsic factors like current blocking grain boundaries and other surface defects is greatly reduced [1-4]. The fundamental limit of R_s is set up by the low frequency BCS surface resistance:

$$R_{BCS} = \omega^2 \frac{A}{T} \exp\left(-\frac{\Delta}{k_B T}\right) + R_i, \quad (1)$$

where Δ is the superconducting gap, and A is a function of superconducting parameters and the mean free path ℓ due to impurities, and R_i is a temperature independent residual resistance [5]. Basically, R_{BCS} is due to the Joule heating of thermally activated normal quasiparticles by the rf electric field $E(x,t) = \mu_0 \omega H_0 \lambda e^{-x/\lambda} \sin \omega t$ induced by the TM01 magnetic field $H_a(t) = H_0 \cos \omega t$ parallel to the cavity surface. For GHz frequencies $\hbar \omega \ll \Delta$ at which Nb cavities operate, $E(x,t)$ and the screening supercurrent density $J(x,t) = (H_0/\lambda) e^{-x/\lambda} \cos \omega t$ are localized in a narrow surface layer determined by the static London penetration depth $\lambda \approx 40$ nm. Recent advances in the cavity technology have resulted in large grain Nb cavities with very high breakdown field $H_b \approx 180$ mT close to the thermodynamic critical field $H_c(0) \approx 200$ mT of Nb. Such fields induce J close to the fundamental depairing limit $J_d = H_c/\lambda$ for which the linear response BCS resistance (1) obtained for $J \ll J_d$ becomes inadequate. In this work we

consider how the quasistatic dependence of $R_s(J)$ on J due to the BCS pairbreaking affects rf thermal breakdown and the behavior of $Q(H_0)$ at intermediate and high fields. We also consider a peculiar nonlinearity of $R_s(H_0)$ due to inhomogeneous thermal breakdown ignited by localized hotspots. The account of these mechanisms can significantly improve the agreement of the thermal feedback model with the observed $Q(H_0)$ curves.

NONLINEAR BCS RESISTANCE

We consider R_s for clean type-II superconductors focusing on the small density of thermally-activated quasiparticles $n(T,J)$ which control R_s . We do not address here effects of impurity scattering and mechanisms of energy relaxation described by complex kinetic equations for quasiparticles and phonons. Instead, we calculate $n(J)$ using the superconducting energy spectrum in a current-carrying state, as shown in Fig. 1:

$$\varepsilon(p) = \sqrt{\Delta^2 + (p - p_F)^2 v_F^2} + \bar{p}_F \bar{v}_s, \quad (2)$$

where the superconducting gap Δ is unaffected by current at $T \ll T_c$, v_F and p_F are the Fermi velocity and momentum, $\mathbf{v}_s = \mathbf{J}/en_0$ is the superfluid velocity, $-e$ is the electron charge, and n_0 is the total density of electrons in the conducting band [6].

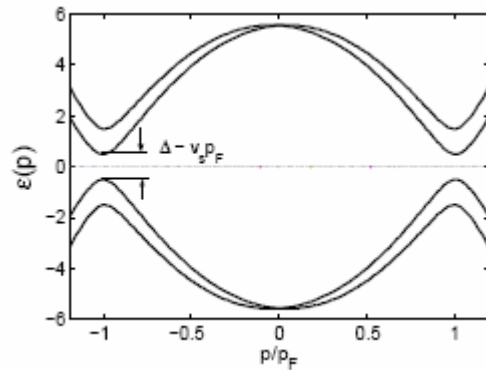


Figure 1. Electron and hole branches of the quasiparticle spectrum $\varepsilon(p)$ in a current-carrying state. The instantaneous $\varepsilon(p,t)$ in rf field with $\omega \ll \Delta$ oscillates between two tilted branches with the effective gap $\Delta_{\text{eff}} = \Delta - v_s p_F$.

The density of thermally-activated quasiparticles $n(J)$ can be calculated by integrating the Boltzmann distribution function, $\exp[-\varepsilon(p)/k_B T]$ over the momentum space:

$$n(J) = \frac{n_{eq}}{2} \int_0^\pi e^{p_F v_s \cos \theta / k_B T} \sin \theta d\theta = n_{eq} \frac{\sinh \beta}{\beta} \quad (3)$$

where $\beta(x,t) = \beta_0 \exp(-x/\lambda) \cos \omega t$, θ is the angle between \mathbf{v}_s and \mathbf{p}_F in Eq. (1), $n_{eq}(T)$ is the equilibrium quasiparticle density, and the parameter β_0 quantifies the effect of low-frequency current on thermal activation:

$$\beta_0 = \frac{v_s p_F}{k_B T} = \frac{\pi}{2^{3/2}} \frac{H_0}{H_c} \frac{\Delta}{k_B T} \quad (4)$$

Here v_s is expressed via the rf field amplitude H_0 and the thermodynamic critical field $H_c = \phi_0 / 2^{3/2} \mu_0 \lambda \xi$, $\xi = \hbar v_F / \pi \Delta$ is the BCS coherence length, and ϕ_0 is the magnetic flux quantum. The rf field thus significantly increases the thermally-activated electron density in Eq. (3) if $\beta_0 \sim 1$, that is, $H_0 \sim TH_c / T_c$. At low temperatures this happens at fields much smaller than H_c , for example for Nb at 2K, $k_B T / \Delta \sim 0.1$, the BCS nonlinearity becomes important for $H_0 \sim 20$ mT. The reason is that the last term in Eq. (2) reduces the gap in the spectrum from Δ to $\Delta_{eff}(v_s) = \Delta - p_F v_s$, which vanishes at the critical velocity $v_c = \Delta / p_F$ above which superconductivity is suppressed by current pairbreaking effects [6]. If expressed in terms of rf field, this condition can be written in the form $H_0 > (2^{3/2} / \pi) H_c \approx 0.9 H_c \approx 180$ mT for Nb. Manifestations of rf current pairbreaking in the nonlinear surface impedance and R_s of clean superconductors were discussed in [7,8].

Nonlinear BCS surface resistance

We now calculate the instantaneous Joule power dissipated in the surface layer of rf field penetration, $q(t) = \int \sigma(v_s) E^2(x,t) dx$, where the nonlinear conductivity $\sigma(v_s)$ is proportional to the normal quasiparticle density $n(v_s)$. Because $n(v_s) / n_0 \propto \exp(-\Delta_{eff} / k_B T)$ is exponentially small, there is no coupling between the rf electric field $E(x,t)$ and $n(v_s)$ which are determined independently by the supercurrent density $J(x,t)$ and the rf field $H_0 \cos \omega t$. In this case the general linear dependence of $\sigma(v_s)$ on $n(v_s)$ can be written in the form, $\sigma(v_s) = \sigma_{BCS} n(v_s) / n_{eq}$, so that for weak rf currents ($\beta_0 \ll 1$), the quasiparticle density n equals the equilibrium density n_{eq} , and the $\sigma(v_s)$ reduces to the linear BCS conductivity. Hence,

$$\frac{q}{H_0^2} = 2R_{BCS} \sin^2 \omega t \int_0^\infty e^{-2x/\lambda} \frac{\sinh(\beta_a e^{-x/\lambda})}{\lambda \beta_a e^{-x/\lambda}} dx \quad (5)$$

where the first factor $e^{-2x/\lambda}$ accounts for the screened profile of $E^2(x)$, the factor $\sinh[\beta(x,t)] / \beta(x,t)$ accounts for the nonuniform distribution of normal quasiparticles $n(\beta)$ as a function of the driving parameter $\beta_a(t) = \beta_0 \cos \omega t$, and

R_{BCS} is the low field BCS surface resistance, so that $q(t) = R_{BCS} H_0^2 \sin^2 \omega t$ for weak fields ($\beta_0 \ll 1$). Performing integration in Eq. (5), we obtain

$$q(t) = 4R_{BCS} H_0^2 \sin^2 \omega t \frac{\sinh^2(\beta_a(t)/2)}{\beta_a^2(t)} \quad (6)$$

Averaging Eq.(6) over the rf period, we calculate the mean rf power $\langle q \rangle$, and then the nonlinear rf surface resistance $R_s(H_0) = 2\langle q \rangle / H_0^2$:

$$R_s = \frac{8R_{BCS}}{\pi \beta_0^2} \int_0^\pi \sinh^2\left(\frac{\beta_0}{2} \cos \tau\right) \tan^2 \tau d\tau, \quad (7)$$

where $\tau = \omega t$. Eq. (7) defines R_s as a function of H_0 both for weak and strong fields. For $\beta_0 \ll 1$, expanding $\sinh(x)$ in series gives the low field $R_s = (1 + \beta_0^2 / 48) R_{BCS}$:

$$R_s \cong \left[1 + \frac{\pi^2}{384} \left(\frac{\Delta}{T}\right)^2 \left(\frac{H_0}{H_c}\right)^2 \right] R_{BCS} \quad (8)$$

Eq. (8) coincides with the result obtained by solving a kinetic equation for quasiparticles to the accuracy of a small logarithmic correction [8]. The pairbreaking nonlinearity becomes more pronounced as T decreases and β increases. For $\beta_0(T) > 1$, the main contribution to the integral (7) comes from a narrow vicinity of the end points $\tau = 0$ and $\tau = \pi$. Then Eq. (7) results in $R_s(H_0)$ exponentially increasing with the rf field:

$$R_s \cong \frac{4R_{BCS} e^{\beta_0}}{\beta_0^3 \sqrt{2\pi\beta_0}} \quad (9)$$

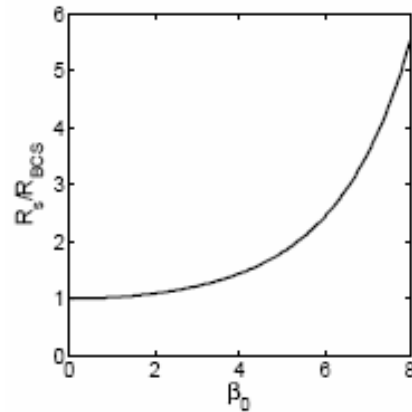


Figure 2: The nonlinear $R_s(\beta_0)$ calculated from Eq. (7).

The full dependence $R_s(\beta_0)$ calculated from Eq. (7) is shown in Figure 2 for the range of β_0 , which corresponds to H_0 from 0 to ≈ 160 mT for Nb at 2K. In this case the

BCS nonlinearity can double R_s at $H_0 \approx 100$ mT as compared to R_{BCS} . For high fields, the surface resistance $R_s \propto \exp[-\Delta_{\text{eff}}(H_0)/k_B T]$ exhibits the Arrhenius exponential temperature dependence with a reduced field-dependent gap $\Delta_{\text{eff}} = (1 - \pi H_0/2^{3/2} H_c) \Delta$ [6-8], which vanishes at the pairbreaking field of $H_0 = 2^{3/2} H_c/\pi$ as shown in Figure 1.

THERMAL RF BREAKDOWN

Uniform thermal breakdown

The exponential temperature dependence of $R_s(T, H_0)$ provides a strong positive feedback between the rf Joule power and heat transport to the coolant, resulting in thermal instability above the breakdown field H_b . The thermal breakdown model [9] is based on the analysis of the heat balance equation for the temperature $T_m(H_0)$ of the cavity surface exposed to rf field:

$$\frac{1}{2} R_s(H_0, T_m) H_0^2 = \frac{(T_m - T_0) \alpha \kappa}{\kappa + d \alpha} \quad (10)$$

Here the left hand side is the rf Joule power and the right hand side is the heat flux to the coolant through the cavity wall of thickness d , where α is the Kapitza thermal conductance between Nb and the coolant held at the temperature T_0 , and κ is the thermal conductivity. As shown in [9], $T_m(H_0)$ slightly increases from T_0 to the maximum value $T_m \approx T_0 + T_0^2/\Delta$ as H_0 increases from 0 to H_b , but for $H_0 > H_b$, stable solutions of Eq. (10) disappear, which indicates thermal runaway.

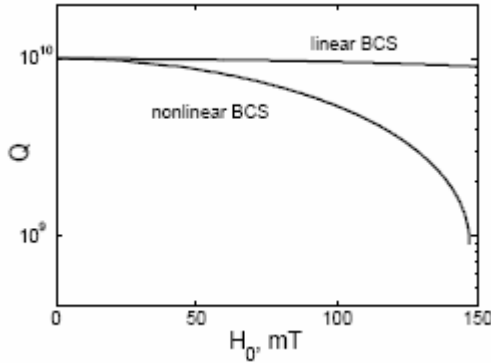


Figure 3. An example of $Q(H_0)$ curves calculated for the linear BCS resistance and the nonlinear R_s given by Eq. (7) for Nb cavity with the parameters given in the text.

To see the effect of the BCS pairbreaking on thermal breakdown, we calculated $Q(H_0)$ for the linear R_{BCS} and the nonlinear $R_s(H_0)$. An example of numerical solution of Eqs. (1), (7) and (10) for Nb is shown in Fig. 3 for 2K, $d = 3$ mm, $\kappa = 20$ mW/mK, $\alpha = 5$ kW/m²K, $R_{BCS} = 10$ n Ω and $Q(0) = 10^{10}$. For $R_i = 0$, the thermal feedback model predicts the breakdown field [9]

$$H_{b0} = \left[\frac{2k_B T_0^2 \alpha \kappa}{(\kappa + d \alpha) \Delta e R_{BCS}} \right]^{1/2}, \quad (11)$$

giving $H_{b0} \sim 300$ mT, well above $H_c = 180$ mT for Nb (here $e = 2.718$). Therefore, if only the linear $R_{BCS}(T)$ is taken into account, this cavity would be stable against thermal runaway up to the fields $H_0 \approx H_c$ at which the surface current density reaches the depairing limit and a superconductor becomes absolutely unstable against vortex penetration. However, the account of the BCS pairbreaking reduces H_b below H_c as evident from Fig. 3. In this case the cavity is stable against vortex penetration, but unstable against uniform thermal breakdown. Another manifestation of the field dependent $R_s(H_0)$ is that the medium and high field Q slopes are significantly increased as compared to the linear R_{BCS} .

Nonuniform thermal breakdown due to hotspots.

The analysis of the previous sections addressed a uniform surface resistance and a global thermal instability, which occurs simultaneously over a significant portion of the cavity surface (at the equatorial region of the highest rf field). However, such idealized instability hardly occurs in real cavities, as has been shown by thermal mapping, which revealed significant localized sources of dissipation (hotspots). Such hotspots cause local temperature peaks of order 0.1-0.3K in macroscopic regions [2-4], as shown in Fig. 4. Given the exponential temperature dependence of R_{BCS} , the hotspots can locally increase rf dissipation by orders of magnitude. Furthermore,

- Hotspots can reduce the global breakdown field because they ignite local thermal quenches [10], which then propagate over the cavity surface.
- Hotspots can significantly increase the medium and high-field Q slopes even for the linear BCS surface resistance, thus masking the fundamental BCS nonlinearity due to rf pairbreaking.

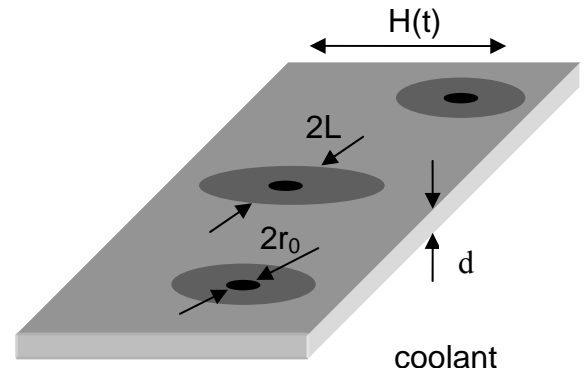


Figure 4. Cavity surface with hotspots (dark grey) caused by smaller defects of radius r_0 (black).

To address these points we consider a steady-state temperature distribution $T(x,y)$ along the cavity surface described by the 2D thermal diffusion equation [10]:

$$d\kappa\nabla^2 T - \alpha_f(T - T_0) + q(T, H_0, r) = 0 \quad (12)$$

Here $T(x,y)$ is averaged over the cavity thickness, $\alpha_f = \alpha/(1 + d\alpha/\kappa)$ is the effective thermal impedance of the cavity wall, and $q = R_s(T, H_0, r)H_0^2/2$ is the rf power which can depend not only on T , but also on the position \mathbf{r} along the surface. For uniform T , Eq. (12) reduces to the heat balance equation (10).

Now we consider what happens if there is a surface domain of radius r_0 where the rf power q is locally enhanced by a defect. Such defects could be grain boundaries, which facilitate local vortex penetration, normal precipitates, nonuniform patches of the oxidized Nb surface or surface steps, which cause local flux concentration [2]. Then the Joule heating term in Eq. (12) can be written in the form, $q(r, T) = q_0(T) + \delta q(r, T)$, where $q_0(T)$ is the uniform Joule power, and $\delta q(r, T)$ is the extra power localized in a small defect region of radius r_0 . Likewise, $T(x,y)$ can be written as $T(x,y) = T_m + \delta T(r)$, where T_m satisfies the uniform heat balance condition $q_0(T_m, H_0) = \alpha_f(T_m - T_0)$, and $\delta T(r)$ is the temperature disturbance due to defect. We consider here weak hotspots, $\delta T_m < k_B T_0^2/\Delta$, for which the nonlinear Eq. (12) can be linearized with respect to the small δT :

$$d\kappa\nabla^2 \delta T - (\alpha_f - q_0')\delta T + \delta q(r) = 0. \quad (13)$$

Here $q_0' = \partial q_0/\partial T$, and all parameters are taken at $T = T_m$. The cylindrically symmetric solution of Eq. (13) is:

$$\delta T(r) = \frac{\Gamma_0}{2\pi d\kappa} K_0\left(\frac{\rho}{L}\right), \quad \Gamma_0 = 2\pi \int_0^{r_0} \delta q r dr, \quad (14)$$

where $K_0(x)$ is a modified Bessel function, $\rho = (r_0^2 + r^2)^{1/2}$, $r_0 \ll L$, Γ_0 is the total extra power generated by the defect, and L is the length, which quantifies the spatial extent of the temperature disturbance in the hotspot:

$$L = \frac{L_h}{\sqrt{1 - q_0'/\alpha_f}}, \quad L_h = \sqrt{\frac{d\kappa}{\alpha_f}} \quad (15)$$

Here L_h is the lateral thermal diffusion length in the absence of the Joule heating. For $d = 3\text{mm}$, $\kappa = 20\text{ W/mK}$, $\alpha_f = 1\text{ kW/m}^2\text{K}$, we obtain $L_h \sim 8\text{ mm}$. The length L is affected by Joule heating, which always increases L as compared to L_h . In fact, $L(H_0)$ diverges if $H_0 \rightarrow H_b$ because $q_0'(H_0) \rightarrow \alpha_f$. For the linear $R_{\text{BCS}}(T)$, we have $q_0' \approx H_0^2 R_{\text{BCS}}(T_m)\Delta/2k_B T^2$, so the term $1 - q_0'/\alpha_f$ in Eq. (15) can be written as $1 - f(H_0)H_0^2/H_b^2$, where $f(H_0)$ varies from $1/e$ at $H_0 \ll H_b$ to 1 at $H_0 \rightarrow H_b$. We illustrate qualitative effects of hotspots on the high-field Q slope for the linear R_{BCS} at $H_0 \sim H_b$, in which case

$$L(H_0) \cong \frac{L_h}{\sqrt{1 - (H_0/H_b)^2}} \quad (16)$$

Here L is the radius of a hotspot on the uniform background $T_m(H_0)$, as shown in Figs. 4 and 5.

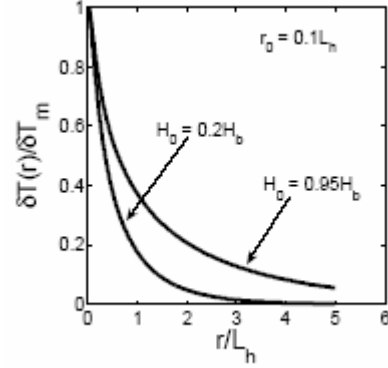


Figure 5. Normalized temperature distributions in hotspots produced by the same defect for different rf fields.

From Eq. (16) it follows that:

1. The hotspot radius $L(H_0)$ can be much greater than either the defect size r_0 and the thermal length L_h . For example, $L \approx 3.2L_h \approx 25.6\text{ mm}$ for $H_0 = 0.95H_b$ and the parameters used above. Since L is independent of r_0 , even a small defect can cause a hotspot much greater than the wall thickness d .
2. $L(H_0)$ increases as H_0 increases, diverging at H_b . Indeed, L is determined by the balance $d\kappa\delta T/L^2 = (\alpha_f - q_0')\delta T$ between lateral heat diffusion and the difference between the heat flux to the coolant $\alpha_f\delta T$ and the Joule power $q_0'\delta T$. As H_0 approaches H_b , the terms α_f and q_0' nearly compensate each other, so it takes more area L^2 to transfer heat from a local source to the coolant. The field dependence of $L(H_0)$ results in a new mechanism of field dependence of the global resistance R_s .

To address the effect of hotspots on R_s we introduce the dimensionless parameter η which quantifies the extra power generated by a defect:

$$\eta = \frac{r_0^2}{L_h^2} \left(\frac{\delta A}{A} + \frac{\delta H^2}{H_0^2} \right) \quad (17)$$

Two terms in the parenthesis represent a local enhancement of the BCS factor A by δA in Eq. (1) and a local field enhancement in the region of radius r_0 , respectively. We consider here only weak local heat sources with $\eta \ll 1$. Notice that for $L_h \sim 8\text{mm}$, all defects with $r_0 < 2\text{mm}$ are weak heat sources even for strong local inhomogeneity, $\delta A \sim A$ or $\delta H^2 \sim H_0^2$. For $r_0 \ll L$, Eq. (14) gives the maximum δT_m in the hotspot:

$$\delta T_m = \frac{\eta}{2}(T_m - T_0) \ln \frac{1.12L}{r_0} \quad (18)$$

The total extra rf power Γ produced by a hotspot can be obtained by integrating Eq. (13) over the surface:

$$\Gamma = 2\pi\alpha_f \int_0^\infty r \delta T(r) dr = \frac{\pi\eta}{2} L^2 H_0^2 R_s(T_m) \quad (19)$$

Summing up Eq. (19) over non overlapping hotspots, we obtain the total dissipation $R_{sg}H_0^2/2$ and hence the global surface resistance R_{sg} :

$$R_{sg}(T, H_0) = \left[1 + \frac{g}{1 - (H_0/H_{b0})^2} \right] R_s \quad (20)$$

where $g = \langle \eta \rangle \pi N_h L_h^2$, N_h is the number of hotspots per unit area, $\langle \eta \rangle$ is the mean value of η , and H_{b0} is the breakdown field for the uniform portion of the cavity. Hotspots can make R_{sg} dependent on H_0 even for low fields if $H_0 \sim H_{b0} \ll H_c$. From Eqs. (10) and (20) we obtain the following parametric dependence of $Q(H_0)$:

$$\frac{2H_0^2}{H_{b0}^2} = 1 + g + u - \sqrt{(1 + g + u)^2 - 4u} \quad (21)$$

$$Q = \frac{Q(0) \exp(-\theta)}{1 + g / [1 - (H_0/H_{b0})^2]}$$

where $\theta = (T_m - T_0)\Delta/k_B T_0^2$, and $u(\theta) = \theta \exp(1 - \theta)$. Here $H_0(\theta)$ is maximum at $\theta = 1$, which defines the global breakdown field H_b reduced by weak hotspots ($g \ll 1$):

$$H_b \approx (1 - 0.5\sqrt{g})H_{b0} \quad (22)$$

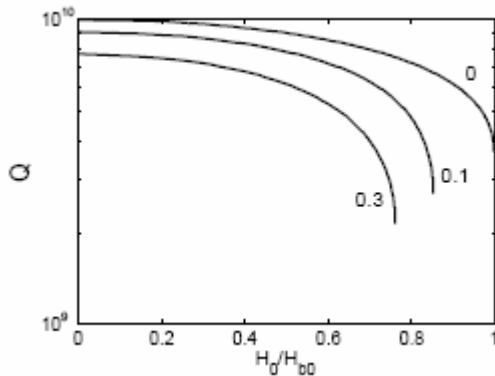


Figure 6. $Q(H_0)$ for the different values of g in Eq. (21): 0 (uniform breakdown), 0.1 and 0.3.

$Q(H_0)$ curves calculated from Eq. (21) are shown in Fig. 6. It is evident that hotspots increase the Q slope because hotspots expand as H_0 increases, resulting in

more rf dissipation at higher fields. The effect of this macroscopic mechanism on $Q(H_0)$ appears similar to that of the BCS nonlinearity shown in Fig. 3. Additional vortex dissipation in hotspots above the penetration field H_p produces kinks on $Q(H_0)$ curves and large high field Q -slope at $H_0 > H_p$ similar to those observed in [11].

DISCUSSION

Both mechanisms of the field dependence of $R_s(H_0)$, considered in this paper manifest themselves in a significant increase of the medium and high field Q slopes and a reduction of the thermal breakdown field H_b below H_c . Although the BCS pairbreaking nonlinearity is controlled by the nanoscale rf surface layer, while hotspot mechanism is basically macroscopic, their manifestations in the behavior of $Q(H_0)$ appear qualitatively similar.

Recent comparison of $Q(H_0)$ curves for cavities from multiple sources with the thermal feedback model based on Eq. (7) has shown that the nonlinear BCS model does capture many essential features of $Q(H_0)$ at frequencies $< 1.5\text{GHz}$ [11]. In particular, the use of Eq. (7) can significantly improve the agreement of the thermal feedback model with experiment as compared to $R_{BCS}(T)$. However, to distinguish the pairbreaking effects from hotspots of grain boundary effects, measurements of $Q(H_0)$ should be combined with T-map measurements, in particular before and after baking. For instance, reduction of the high field Q slope is consistent with the assumption that baking may remove or ameliorate some of hotspots.

Application of Eq. (7), obtained for clean type-II superconductors, to Nb cavities critically depends on the information about impurity scattering in the 40 nm surface layer. Such data are still lacking, though first measurements of impurity profiles using atom probe tomography [12] and SXRD [13] were recently reported. Generally, impurity scattering reduces the pairbreaking nonlinearity of $R_s(H_0)$, so making the Nb surface layer dirtier may reduce Q slope and increase H_b . Such clean to dirty transition may be responsible for reducing Q slope after baking, particularly for big grain Nb cavities with high $H_b \approx 180\text{ mT}$ [3].

REFERENCES

- [1] D. Proch, Rep. Prog. Phys. **61**, 431 (1998).
- [2] H. Padamsee, Supercond. Sci. Technol. **14**, R28 (2001).
- [3] P. Kneisel, G. Ciovati, G. Myneni, J. Sekutowicz, T. Carneiro, this conference.
- [4] K. Saito, this conference.
- [5] J.P. Turneaure, J. Halbritter, and H.A. Schwettman, J. Supercond. **4**, 341 (1991).
- [6] J. Bardeen, Rev. Mod. Phys. **34**, 667 (1962).
- [7] M.P. Garfunkel, Phys. Rev. **173**, 516 (1968).
- [8] I. Kulik and V. Palmieri, Special Issue of Particle Accelerators, **60**, 257 (1998).
- [9] A. Gurevich, Pushing the Limits of RF Superconductivity workshop, ANL, Sept 22-24 2004

- [10] A. Gurevich and R.G. Mints, Rev. Mod. Phys. **59**, 941 (1987).
- [11] P. Bauer, N. Solyak, G.L. Giovati, G. Ereemeev, A. Gurevich, L. Lilje, B. Visentin, this conference.
- [12] D.N. Seidman, J.T. Sebastian, J. Norem, and P. Bauer, this conference.
- [13] M. Delheusy, A. Stierie, C. Antonie, N. Kasper, I. Costina, H. Dosch, this conference.